

Article

Possible Synthetic Approaches for Heterobimetallic Complexes by Using *n*NHC/*tz*NHC Heteroditopic Carbene Ligands

Andrea Longhi ¹, Marco Baron ¹, Marzio Rancan ², Gregorio Bottaro ², Lidia Armelao ^{1,2}, Paolo Sgarbossa ³ and Cristina Tubaro ^{1,*}

- ¹ Department of Chemical Sciences, University of Padova, via F. Marzolo 1, 35131 Padova, Italy; andrea.longhi.1@phd.unipd.it (A.L.); marco.baron@unipd.it (M.B.); lidia.armelao@unipd.it (L.A.)
- ² Institute of Condensed Matter Chemistry and Technologies for Energy, National Research Council, ICMATE-CNR, c/o Department of Chemical Sciences, University of Padova, via F. Marzolo 1, 35131 Padova, Italy; marzio.rancan@cnr.it (M.R.); gregorio.bottaro@cnr.it (G.B.)
- ³ Department of Industrial Engineering, University of Padova, via F. Marzolo 9, 35131 Padova, Italy; paolo.sgarbossa@unipd.it
- * Correspondence: cristina.tubaro@unipd.it; Tel.: +39-049-8275655

Academic Editor: Rajendra S. Ghadwal

Received: 16 May 2019; Accepted: 11 June 2019; Published: 21 June 2019



Abstract: The synthesis of heterobimetallic complexes remains a synthetic challenge in the field of organometallic chemistry. A possible approach in this regard might be the use of a bidentate heteroditopic bis(carbene) ligand that combines an imidazol-2-ylidene (*n*NHC) with a 1,2,3-triazol-5-ylidene (*tz*NHC) connected by an organic spacer. The optimized strategy to heterobimetallic complexes with this type of ligand involves a 3-step procedure: (i) Coordination of the *n*NHC, functionalized with a 1,2,3-triazole ring, to a metal center; (ii) formation of the triazolium ring by alkylation of the triazole N-3; (iii) deprotonation of the *tz*NHC precursor and coordination of the second metal center. Following this procedure, a novel Au(I)-Ag(I) dinuclear complex was isolated and its properties were compared to the analogous homobimetallic Ag(I)-Ag(I) and Au(I)-Au(I) complexes. The study was completed by the determination of the molecular structures of some synthetic intermediates.

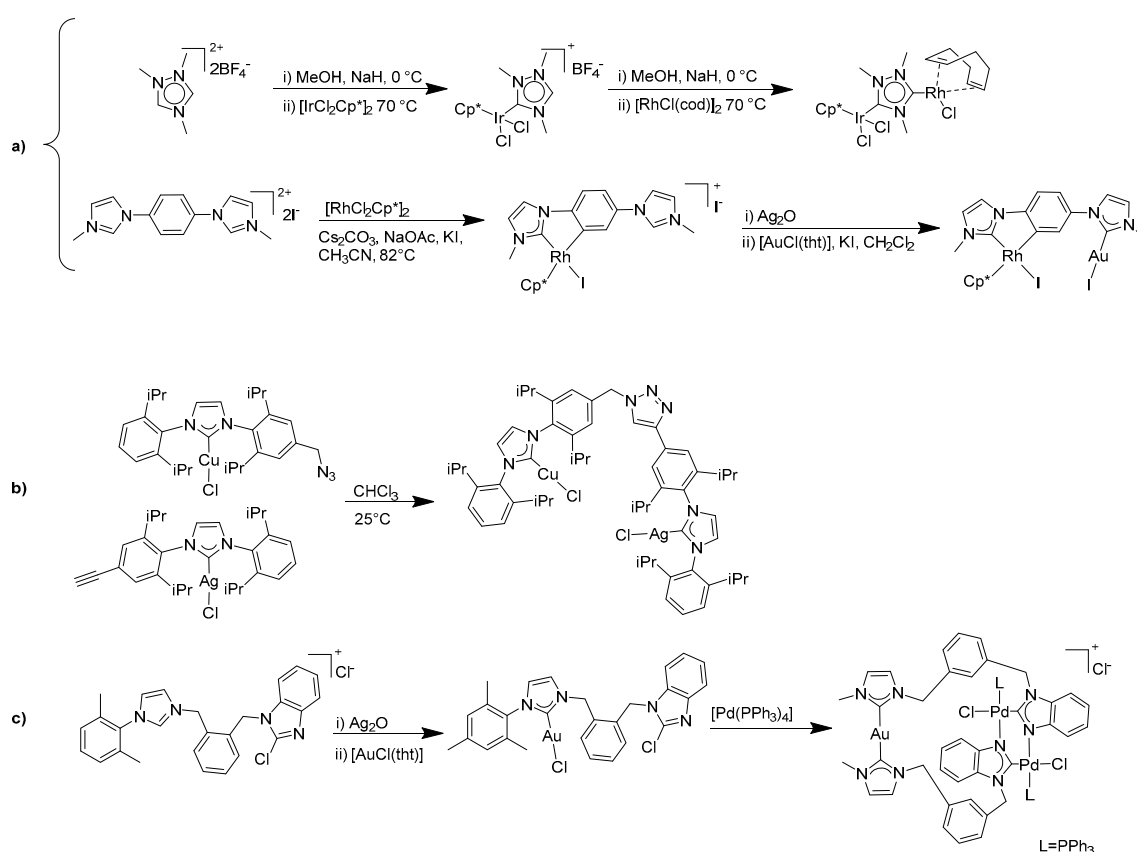
Keywords: gold(I) complexes; NHC ligands; *abnormal* NHC ligands; heteroditopic ligands

1. Introduction

Since the first report by Arduengo on an isolable N-heterocyclic carbene (NHC) in 1991 [1], this class of compounds has become widely popular in coordination chemistry [2–4]. Among the assets of NHCs as ligands, we find the high stability of their metal complexes, due to the strength of the carbene-metal bond, the possibility of easily introducing functional groups in their structure and the tuning of the steric and electronic properties of the metal center by varying the nature and the properties of the heterocyclic ring. NHC metal complexes find thus application in homogeneous catalysis [5–7], in the preparation of luminescent [8] and liquid crystalline materials [9] and as metallodrugs [10–12].

Aiming to preparing very stable complexes, an additional possibility, is the use of bidentate carbenes, enabling chelating or bridging coordination mode of the ligand [13]. In this regard, the possibility of preparing dinuclear complexes is of particular interest in the case of linearly dicoordinated d^{10} metal centers, which are known to present metal-metal interactions, the so-called metallophilic interaction. The aurophilic interaction between gold(I) centers, introduced by Schmidbaur [14], is the most famous phenomenon of this type, and its presence, together with the relativistic effects distinctive of gold, might be connected with high-quality emission properties [15–17].

Another interesting opportunity with bidentate ligands is the possibility to synthesize homo- or heterobimetallic complexes. The possibility of combining different metals in one compound is particularly fascinating in the field of homogeneous catalysis, allowing in principle cooperativity effects between metal centers with different electronic and coordination properties. Heterobimetallic catalysis is thus an emerging research area [18], whose development is, however, slowed down by a non-trivial synthetic problem, namely a straightforward and rational synthesis of heterobimetallic complexes. The synthesis and catalytic application of heterobimetallic complexes bearing NHC donors have been reviewed five years ago by Peris and Hahn [18] and more recent examples have been reported by the same authors [19–22], as well as by other ones [23,24]. Although successful synthetic approaches are present in the literature, the majority of them is not general and works only in specific conditions. For example, the stepwise metalation of polycarbene ligands has been successfully employed in several cases (Scheme 1a), although the coordination of two different metal centers is driven by the geometrical constraints of the ligand and by the different coordination geometries of the investigated metal centers [25]. In other cases, two metal complexes are linked via post-functionalization of the carbene ligands, for example by formation of a new heterocyclic ring (namely the 1,2,3-triazole) (Scheme 1b) [26]. Finally, Hahn and co-workers have recently reported a procedure based on a bis-NHC precursor in which the two heterocyclic rings can be coordinated to the two metal centers, via different reactions, i.e., deprotonation of the azolium salt and oxidative addition of the C-Cl bond (Scheme 1c) [27].



Scheme 1. Examples of possible strategies for the isolation of heterobimetallic complexes reported in the literature and described in the text: (a) stepwise metalation of polycarbene ligands; (b) linking of metal complexes via post-functionalization of carbene ligands; (c) coordination of two metals via two different reactions (deprotonation of the azolium salt and oxidative addition).

We have recently reported an $n\text{NHC}-t\text{zNHC}$ heteroditopic ligand with a propylene linker between the two carbene donors [28]; considering the synthetic procedure to obtain the ligand precursor,

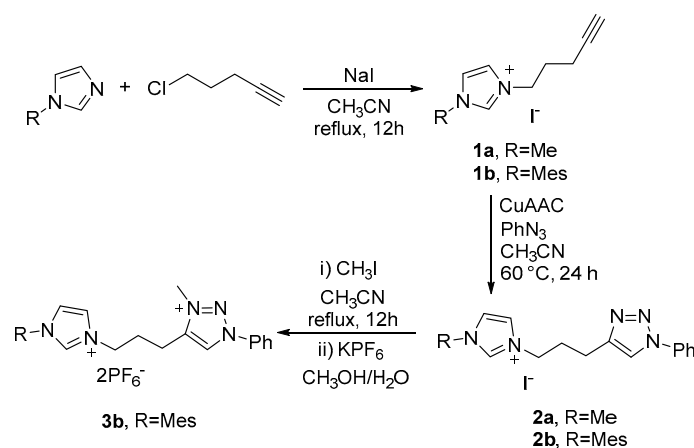
we embarked on the investigation of a rational stepwise synthetic procedure for the isolation of heterobimetallic complexes with this type of ligand. A very similar *n*NHC-*tz*NHC ligand (with a shorter linker between the carbene units) was used by Cowie et al. in the synthesis of a Pd(II)/Rh(I) heterobimetallic complex in a stepwise metalation approach [29], exploiting the different acidic properties of the two azole rings [30]. They recognized indeed that the outcome of the reaction was not general, toughly depending on the used metal precursors.

Here, we report on our attempts to isolate heterobimetallic complexes, following different synthetic approaches, dealing mainly with the post-functionalization of an already coordinated carbene ligand. It can be anticipated that a novel silver(I)-gold(I) heterobimetallic complex has been isolated and characterized, together with its homobimetallic analogues. Moreover, mononuclear gold(I) complexes, intermediates in the synthetic procedure, have been fully characterized by means of ^1H and ^{13}C -NMR, ESI-MS and single-crystal X-ray structure.

2. Results and Discussion

2.1. Synthesis of the Proligands

Alkynyl-imidazolium salts **1a,b** were synthesized using a slightly modified procedure reported in the literature for similar compounds [31], which involves a nucleophilic substitution reaction between an N-substituted imidazole and 5-chloro-1-pentyne in acetonitrile under reflux (Scheme 2).



Scheme 2. Synthesis of the imidazolium salts **1a,b**, **2a,b** and **3b**.

Products **1a,b** were synthesized in high yield and their formation was confirmed by the ^1H -NMR spectra (see Supplementary Material), which present the characteristic imidazolium C2-H proton at ca. 9.7 ppm. The 1,2,3-triazole moiety was then obtained via the common copper azido-alkyne 1,3-dipolar cycloaddition (CuAAC), although a stoichiometric amount of Cu(II) and sodium ascorbate was required (Scheme 2) [32]. The success of the reaction can be easily checked with the ^1H -NMR spectra, which present multiplets in the range 7.3–7.9 ppm, associable to the phenyl ring protons, and a new signal at δ ca. 8.0 ppm attributable to the proton in position 5 of the triazole ring. Finally, the ESI-MS spectra show the fragments corresponding to the cationic part of the salt at m/z 268.05 and 372.08 for **2a** and **2b** respectively. Considering the significant amount of copper, the imidazolium salts **2a,b** must be carefully purified, in order to remove all the copper species, thus avoiding possible side reactions during the synthesis of the complexes (see further in the text in Section 2.2).

Imidazolium salts **2a,b** are precursors of mono-*n*NHC ligands, since only the imidazolium functionality could be deprotonated to give a carbene. Only the quaternization of the N-3 triazole position with an alkyl group affords a triazolium salt, which upon deprotonation of the CH in position 5 of the ring, could give a second carbene fragment. In this view, proligand **3b** was isolated by methylation of **2b** with excess MeI in acetonitrile under reflux for 12 h, followed by I^-/PF_6^- anion

exchange in a MeOH/H₂O mixture. The ¹H-NMR spectrum confirms the methylation of the nitrogen atom. In particular, the CH in position 5 of the triazole moves downfield at δ 8.72 ppm close to the signal of the procarbenic proton of the imidazole ring; furthermore, a singlet appears at δ 4.26 ppm, attributable to the methyl protons. The ESI-MS spectra show a peak at 532.08 *m/z* associated with [3b-PF₆]⁺ fragment. By slow diffusion of diethyl ether into an acetonitrile solution of 3b, some crystals suitable for X-ray single crystal diffraction analysis were obtained. The X-ray crystal structure confirms the nature of 3b (Figure 1) as an imidazolium/triazolium salt.

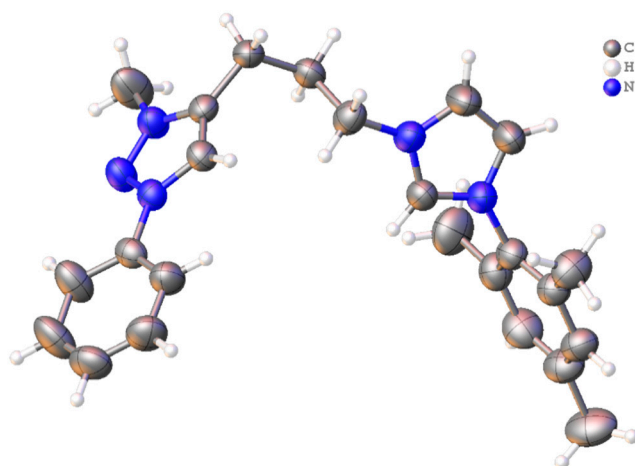
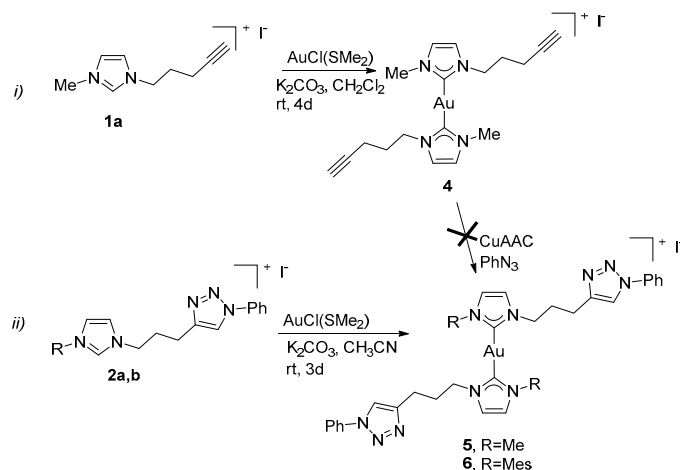


Figure 1. ORTEP view of the cationic part in compound 3b. Ellipsoids are drawn at 50% probability. PF₆[−] anions are omitted for clarity.

2.2. Synthesis and Properties of Mononuclear Gold(I) Complexes

Considering the proligands described in the previous section, different procedures could be adopted for the synthesis of the gold(I) complexes, as summarized in Scheme 3. In particular, the formation of the triazole ring can occur after the coordination of the imidazol-2-ylidene to the gold center (path *i*) or before it (path *ii*).



Scheme 3. Synthesis of the gold(I) complexes 4–6.

Complex 4 was isolated in good yield by the reaction of the alkynyl-functionalized imidazolium salt 1a with AuCl(SMe₂) in a 2:1 molar ratio, in the presence of a weak base (K₂CO₃) under an inert atmosphere and mild conditions (room temperature in dichloromethane for 4 days). The identity of complex 4 was confirmed by ESI-MS spectra which show a peak at *m/z* 493.12 relative to the cationic

part of the complex $[\text{AuL}_2]^+$ ($\text{L} = \text{NHC}$). In the ^{13}C -NMR spectrum, the signal at δ 185.0 ppm is attributed to the C2-imidazole carbene coordinated to the gold(I) center [33]. The definitive support for the proposed structure comes from the single crystal X-ray diffraction analysis (Figure 2).

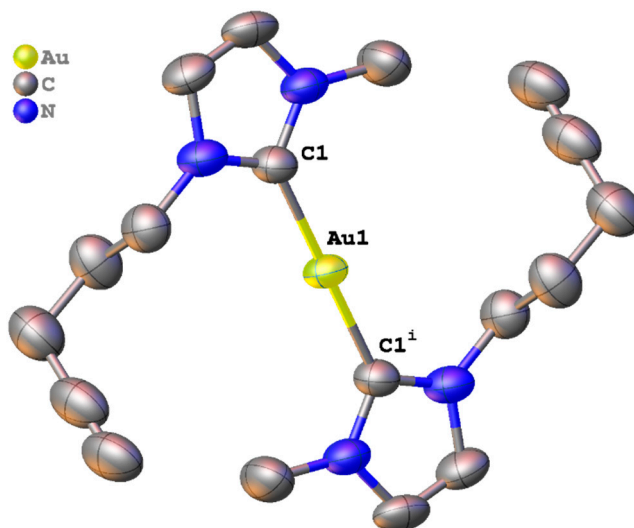


Figure 2. ORTEP view of the complex cation in compound 4. Ellipsoids are drawn at 50% probability. Hydrogen atoms and iodide anion are omitted for clarity. Selected bond distances and angles: Au1—C1 2.031(6) Å and C1—Au1—C1ⁱ 180°. Symmetry operation $i = 1 - x, 1 - y, 1 - z$.

As expected for a d^{10} metal center, gold(I) has a linear coordination geometry. The carbene–Au(I) bond distance (2.031(6) Å) is comparable with the values observed in the literature for other $[\text{Au}(\text{NHC})_2]\text{X}$ complexes [33]. The complex has an *anti* conformation, i.e., the bulkiest substituents of the two ligands lay on opposite sides with respect the C1—Au1—C1ⁱ line. The alkyne functional groups in complex 4 could react with an azide to form the triazole moiety (path *i*, Scheme 3), however, in all the performed attempts, decomposition of complex 4 has been observed.

For the described problems, procedure *ii* (Scheme 2) was therefore adopted. The reaction between two equivalents of proligand 2a (or 2b), presenting a triazole pendant group, with AuCl(SMe₂) in acetonitrile using K₂CO₃ as the base was performed (Scheme 2), affording the bis(NHC) complex 5 (or 6) [34]. The ^{13}C -NMR spectra show a signal at δ 184.8 or 184.9 ppm, for 5 and 6 respectively, in the typical range of carbene carbons coordinated to a gold(I) center [33]. The ESI-MS spectra show peaks at 731.23 or 939.27 *m/z*, for 5 and 6 respectively, associated with the loss of the iodide counter anion from the complex. This supports the formation of the gold(I) bis-carbene complex. Crystals of complex 6 suitable for the single crystal X-ray diffraction were obtained by slow diffusion of diethyl ether into an oily suspension of complex 6 in an acetonitrile/hexane mixture. The X-ray structure confirms the formation of the bis-carbene gold(I) complex (Figure 3).

The two carbene–Au(I) distances (2.006 and 2.010 Å, respectively) are comparable with those reported in the literature for other bis-carbene Au(I) complexes [33]. Also in this case, the two ligands adopt an *anti* conformation.

When using an impure batch of proligand 2a, the solid isolated at the end of the synthesis was red colored, while normally the Au(I) NHC complexes are white or off-white solids. Moreover, the ^1H -NMR spectrum of this solid shows the presence of two main sets of signals (in ca. 1/1 ratio), one of which associable to complex 5. The nature of the second species, complex 7, was fully clarified thanks to single crystal X-ray diffraction analysis. The compound is an Au(III) complex (Figure 4) with a square planar geometry, as expected for d^8 metal center, where two NHC ligands and two iodide anions coordinate the metal. A third, uncoordinated, iodide anion is present for charge balance reasons.

The obtained isomer is the *trans* one, as already observed in other I₂ oxidative addition reactions to gold(I) centers [35].

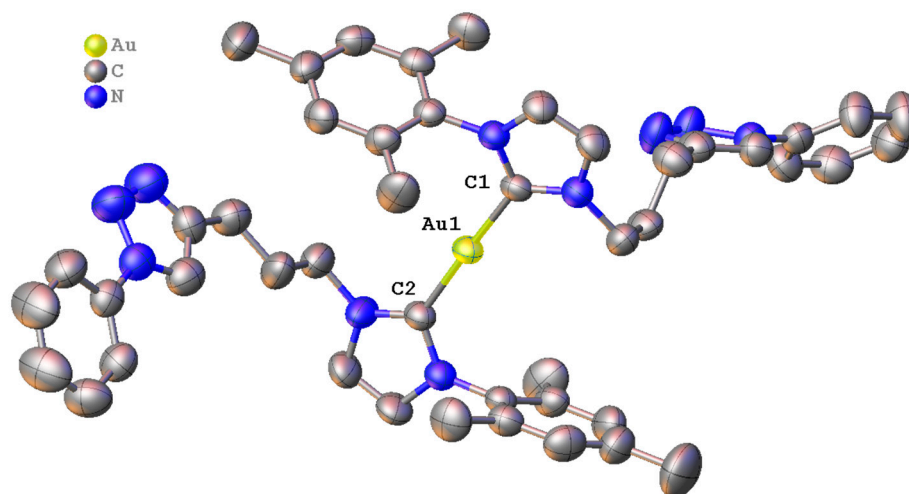


Figure 3. ORTEP view of the complex cation in compound 6. Ellipsoids are drawn at 50% probability. Hydrogen atoms and iodine anion are omitted for clarity. Selected bond distances and angles: Au1—C1 2.006(4) Å, Au1—C2 2.010(4) Å and C1—Au1—C2 176.90(16)°.

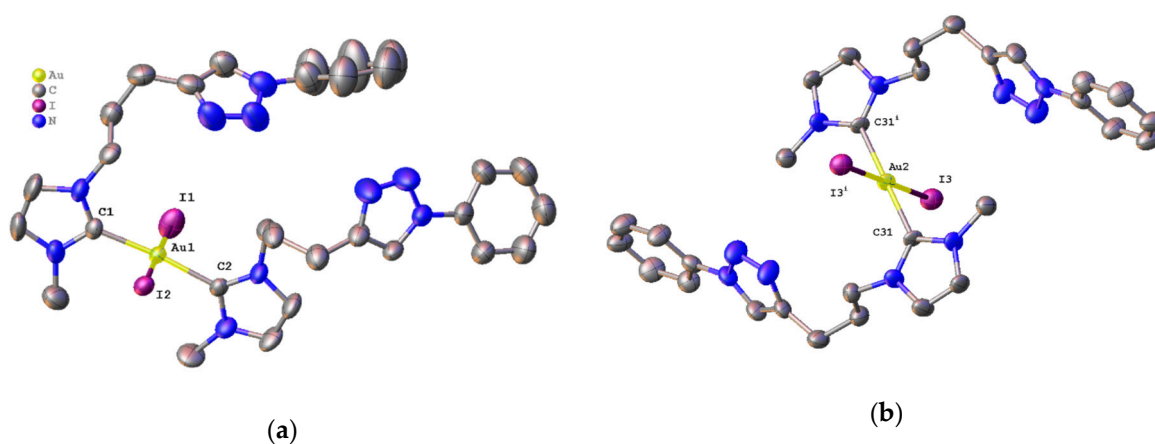


Figure 4. ORTEP view of the complex cation in compound 7. Ellipsoids are drawn at 50% probability. Hydrogen atoms and uncoordinated iodide anions are omitted for clarity. Two conformational isomers are present in the unit cell: (a) The *syn* species, (b) the *anti* one. Selected bond distances and angles: Au1—C1 2.030(11) Å, Au1—C2 2.047(11) Å, Au1—I1 2.6390(10) Å, Au1—I2 2.6324(9) Å, Au2—C31 2.050(10) Å, Au2—I3 2.6409(9) Å and C1—Au1—C2 174.3(4)°, I1—Au1—I2 179.59(4)°, C31—Au2—C31ⁱ 180°, I3—Au2—I3ⁱ 180.00(3)°. Symmetry operation $i = 1 - x, 1 - y, 1 - z$.

Very interestingly, in the crystal, contrary to what found in the case of complexes 4 and 6, two crystallographic independent conformational isomers (*syn* and *anti*) can be found. Figure 4a shows the *syn* conformation while the *anti* one is depicted in Figure 4b. The geometry of the *syn* isomer is slightly deformed from ideal angles values (for instance: C1—Au1—C2 174.3(4)°), probably because of the steric repulsion between the bulky substituents.

The packing in the crystal consists of the repetition of *syn-anti-syn* layers. Between each *syn* layers, there are uncoordinated iodide anions interacting with iodides bonded to the gold(III) centers forming the following connectivity I—Au—I⋯I—Au—I, with I⋯I distances of 3.4170(7) Å. In the case of the *anti* isomer, the interactions involving the metal and the iodide anions (coordinated and not) give connectivity of the type I⋯I—Au—I⋯I, with I⋯I distances of 3.6973(13) Å (Figure 5). The presence of these

I...I interactions could justify the stabilization in the crystal lattice of the *syn* isomer, that should have higher energy because of the major steric repulsions between the NHC chains, when compared to the *anti* species.

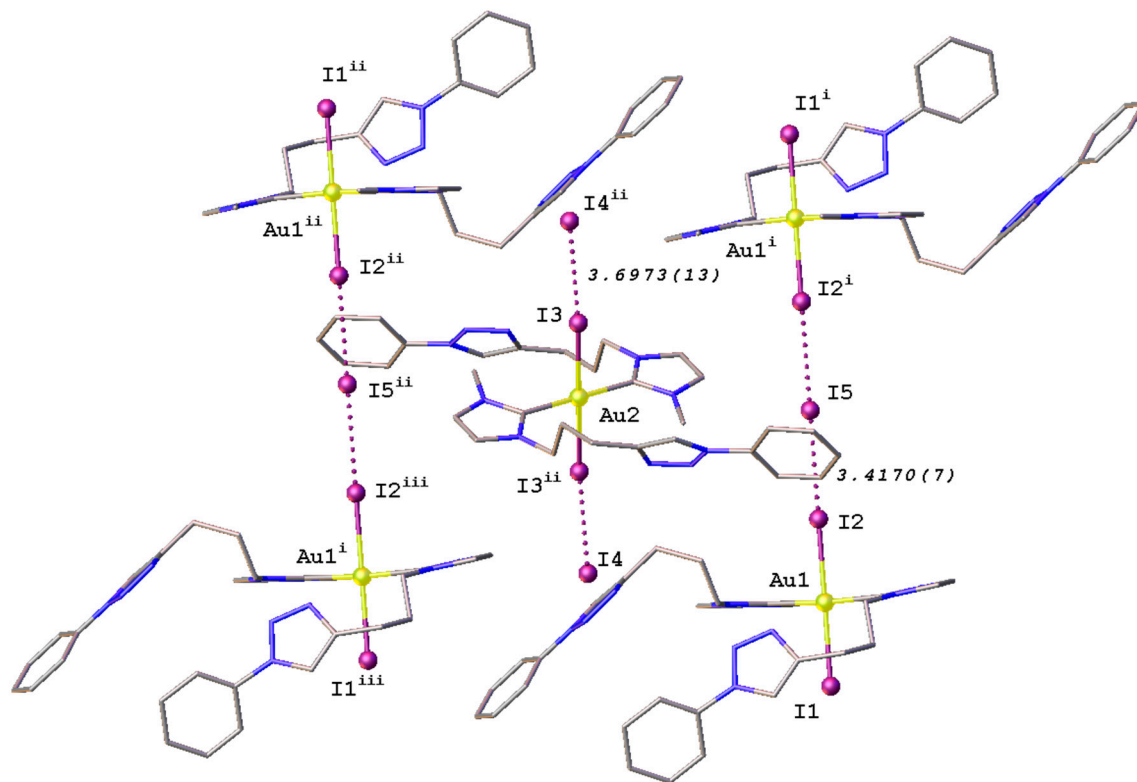


Figure 5. Packing in the crystal of complex 7, with the repetition of *syn-anti-syn* layers. Symmetry operations $i = -x, -y, 1 - z$; $ii = 1 - x, 1 - y, 1 - z$; $iii = 1 + x, 1 + y, z$.

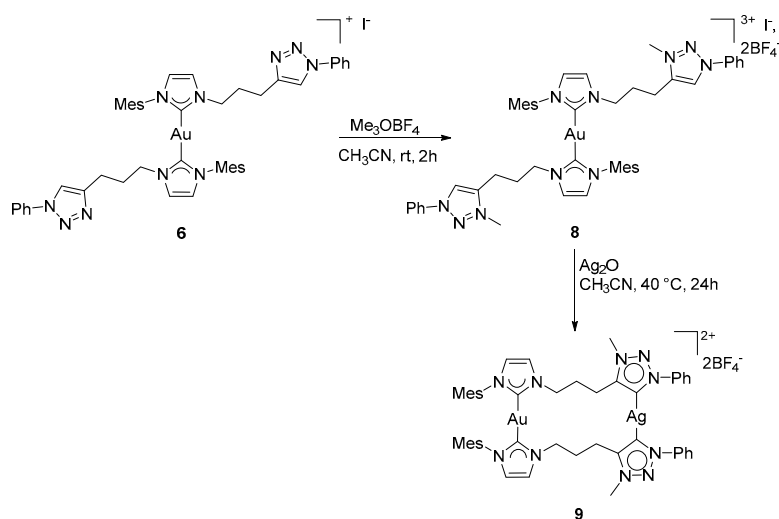
The oxidation to Au(III) could be correlated to the presence of impurities of copper species still present in the ligand precursor. In fact, it is well known that Cu(II) can oxidize iodide to iodine and that iodine can then oxidize gold(I) to gold(III).

In the NMR spectra, the signals associated with complex 7 are very similar (in number and multiplicity) to those detected for complex 5, although slightly shifted to higher ppm, as expected for a complex in which the metal center has a higher Lewis acid character.

2.3. Synthesis and Properties of Dinuclear Complexes

In view of isolating heterobimetallic complexes, the alkylation of the N-3 position of the triazole ring is required, so that upon deprotonation of C5-H, a second carbene ligand can be obtained. The stepwise methylation approach was also adopted by Barnard and coworkers for the isolation of dinuclear heterobimetallic complexes having two bridging di-*n*NHC ligands [36].

Complex 6 was therefore converted to complex 8 by using a strong methylating agent, the Meerwein salt Me₃OBF₄, in 2 h in acetonitrile solution (Scheme 4). Other methylating agents, like for example MeI do not afford any product; this is not surprising considering that also in the literature it is reported that strong alkylating agents should be used in the case of triazole rings [28].



Scheme 4. Synthesis of complexes 8 and 9.

The formation of complex 8 can be confirmed by the $^1\text{H-NMR}$ spectrum, in which a new methyl signal at δ 4.20 ppm appears; furthermore, the triazole C5-H results deshielded from δ 8.11 to 8.74 ppm, due to the positive charge on the ring. The $^{13}\text{C-NMR}$ spectrum shows the new CH_3 signal at δ 38.6 ppm, without losing the carbene signal at 184.9 ppm. The ESI-MS presented the peak at m/z 1143.33 associated with the fragment $[\mathbf{8-I}]^+$ (loss of an iodide anion).

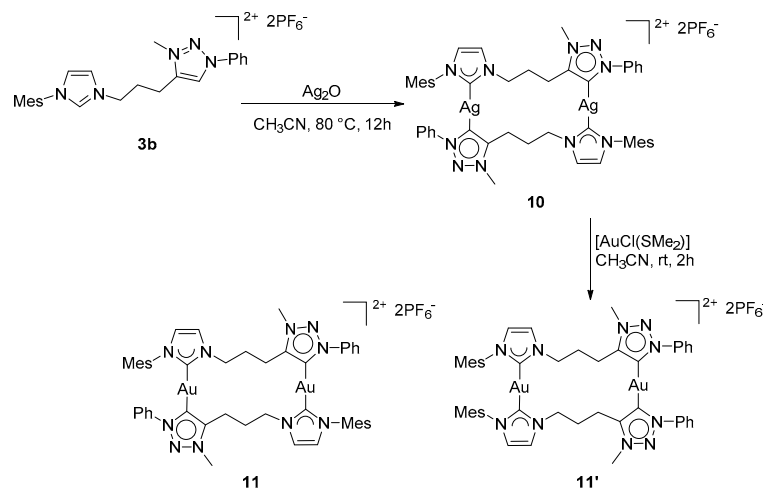
Complex 8 was reacted with Ag_2O in acetonitrile, heating the mixture at 40°C in a pressure tube for 24 h (Scheme 4). In the $^1\text{H-NMR}$ spectrum of complex 9, it is possible to observe the disappearance of the C5-H signal; this suggests the deprotonation of the triazolium ring to form the carbene ligand. The $^{13}\text{C-NMR}$ spectrum shows two carbene signals, at 184.0 for the $\text{C}_{\text{im-Au}}$ and 165.1 for the $\text{C}_{\text{tz-Ag}}$; the chemical shift of these signals is comparable with those reported in the literature for imidazol-2-ylidene and 1,2,3-triazol-5-ylidene ligands coordinated to gold(I) [15,33,37] and silver(I) [38,39] centers respectively. Furthermore, similar chemical shifts were observed for the previously synthesized homobimetallic Au(I)-Au(I) and Ag(I)-Ag(I) complexes having an analogous ditopic *n*NHC-*tz*NHC ligand [28]. As expected the mesoionic carbene carbon (C_{tz}) has a lower chemical shift than the *normal* carbene (C_{im}), indicative of superior donor properties [40–42]. The ESI-MS spectra show the signal at 1163.25 m/z associated with the fragment $[\mathbf{9-BF}_4]^+$ and the simulated isotopic pattern clearly matches the experimental one. Complex 9 evidenced a moderate tendency to decomposition (both in solution and solid state) developing a dark color, probably due to the formation of metallic aggregates, after few days of exposure to light at ambient atmosphere. Interestingly, complex 9 might represent the precursor of others heterobimetallic complexes and we report here only the transmetalation to gold(I). The results obtained in this reaction are particularly helpful for the identification of one of the homobimetallic gold species (see further in the text) and for this reason, they will be discussed in the next paragraph.

To compare the properties of the heterobimetallic complex 9, its homobimetallic silver(I) and gold(I) analogues were synthesized, following already reported procedures (Scheme 5).

The dinuclear homobimetallic silver(I) complex 10 was isolated by the reaction of the bis(azolium) salt 3b with silver(I) oxide in acetonitrile at 80°C . The identity of the silver(I) complex as a dinuclear dicationic species with two bridging di(N-heterocyclic carbene) ligands has been supported by the disappearance of the two signals at ca. 8.5 ppm suggesting the deprotonation of the diazolium salt and by the ESI-MS spectrum showing the fragment $[\mathbf{10-PF}_6]^+$ at 1131.04 m/z .

Subsequently, the gold(I) complex was synthesized by transmetalation reaction between the silver complex 10 and $\text{AuCl}(\text{SMe}_2)$ in acetonitrile as a solvent, using an Ag: Au ratio ca. 1:1. In this case, two sets of signals are present in the $^1\text{H-NMR}$ spectra in a 1:1 ratio, associable to two constitutional

isomers of the gold(I) complex; in particular, we have recently reported and commented on this regard, concluding that the two isomers are associable to the head-to-head or head-to-tail coordination of the heteroditopic ligand [28]. We have labeled the crude mixture of complexes isolated at the end of the synthesis **11/11'** with the apostrophe indicating the head-to-head coordination of the ligand. In the ESI-MS spectrum, the mixture **11/11'** shows a signal at 1309.23 m/z corresponding to the loss of one PF_6^- anion from the complex.



Scheme 5. Synthesis of the dinuclear silver(I) complex **10** and of the gold(I) complexes **11** and **11'**.

The gold(I) isomers could be separated by slow diffusion of diethyl ether into an acetonitrile solution of the mixture. In particular, it was possible to isolate few crystals of the less soluble isomer **11**, suitable for single crystal XRD analysis. The solved structure (Figure 6) shows the head-to-tail coordination of the ligand with a stretched conformation of the bridge. The two gold centers stand at the distance of 6.2 Å, thus the presence of auriphilic interaction can be excluded in this compound. Bond distances of the metal coordination sphere are very similar to what is found in the other Au compounds here presented, while the coordination geometry of the gold center is slightly deformed from ideal angles values (C1—Au1—C13^i $173.78(4)^\circ$), probably because of structural constrains imposed by the cyclic structure.

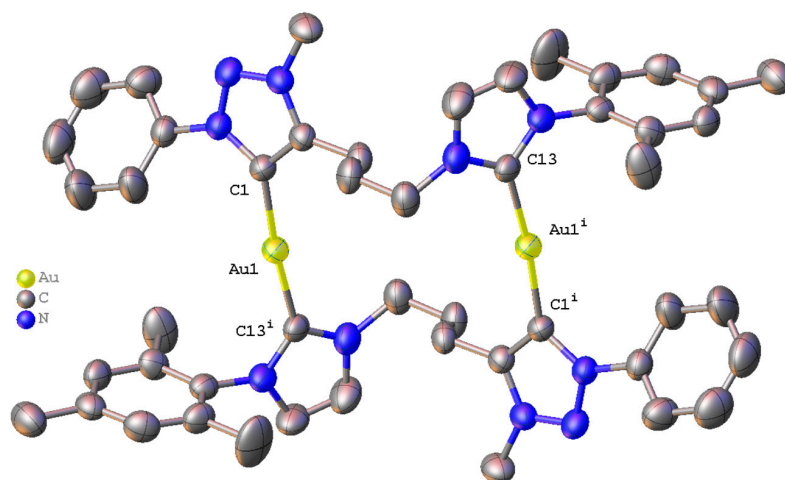


Figure 6. ORTEP view of the complex cation in compound **11**. Ellipsoids are drawn at 50% probability. PF_6^- anions and hydrogen atoms are omitted for clarity. Selected bond distances and angles: Au1—C1 $2.028(5)$ Å, Au1—C13^i $2.027(5)$ Å, and C1—Au1—C13^i $173.78(4)^\circ$. Symmetry operation $i = 1 - x, 1 - y, 1 - z$.

An indirect proof of the identity of complex **11'** as dinuclear gold(I) complex with the two bridging dicarbene ligands coordinated in head-to-head coordination, comes from the Ag-Au transmetalation reaction starting from complex **9**, in which the head-to-head coordination of the ligand is imposed by the synthetic procedure. We added a slight excess of AuCl(SMe₂) to the solution of complex **9** in deuterated acetonitrile and followed the reaction via ¹H-NMR spectra. The transmetalation reaction is accompanied by the formation of an off-white precipitate (the insoluble AgCl) and, as evidenced by the spectra reported in Figure 7, the main product of the reaction is complex **11'**. In fact, the diagnostic signals of complex **11'** (indicated with a red line) are practically coincident with those of the species present in the NMR reaction mixture. Moreover, the chemical shifts of the signals associated with complex **11'** are very close to those of complex **9**, that should present a very similar structure. This is not surprising because it is well known that the substitution of Ag atoms with Au ones in NHC complexes has a negligible influence in the position of the proton NMR signals.

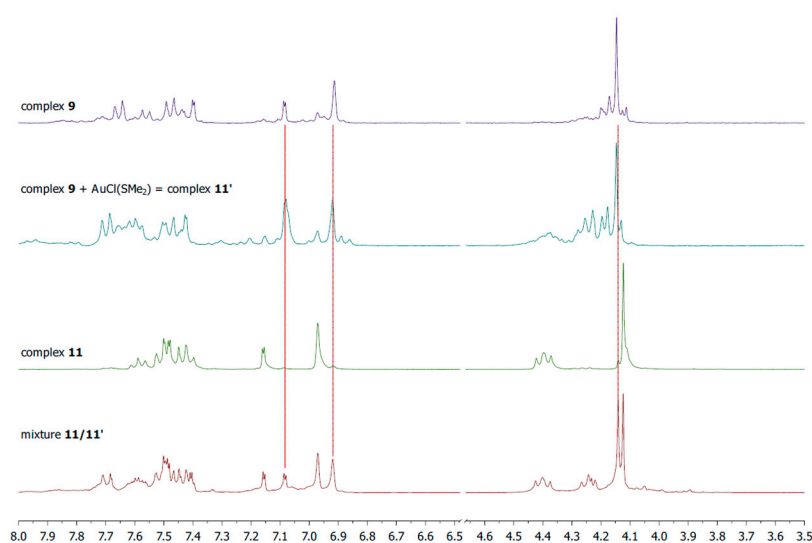


Figure 7. ¹H-NMR spectra in deuterated acetonitrile of complex **9** (purple spectrum), complex **9** + excess of AuCl(SMe₂) (blue spectrum), complex **11** (green spectrum) and mixture **11/11'** in 1/1 ratio, isolated with the procedure described in Scheme 5 (red spectrum).

2.4. Luminescence Properties

The room temperature emission spectra of the **3b** ligand and of **9**, **10**, **11** and **11'** complexes were obtained from films prepared drop-casting acetonitrile solutions of the different compounds onto silica slides (Figure 8). The photoluminescence spectra of the complexes are red-shifted compared with that of the diazolium salt **3b** (emission λ_{\max} 335 nm) precursor of the *n*NHC-*tz*NHC ligand. The observed shift is ascribed to the metal coordination which causes a perturbation on the molecular orbitals as often happen in this kind of noble metal complexes [15,28,43,44]. All the dinuclear complexes have emission maxima in the blue-region between 400–440 nm (λ_{\max} = 395 for **9**; 412 for **11** and **11'** and 435 nm for **10**). Besides for the position of the emission maxima, the PL spectra of **9**, **10**, **11** and **11'** show a different broadening in the long wavelength side that induce a color shift toward the white region of the CIE1931 chromaticity diagram.

The spectra of **11** and **11'** are similar to those of the analogue homobimetallic complex [Au₂{MeIm(CH₂)₃*tz*NHC}₂](PF₆)₂ having a methyl as wingtip group on the *N*-imidazole ring instead of a mesityl one [28]. Moreover, it is interesting to underline that the emission λ_{\max} in complex **11** is blue-shifted compared to that of the complex [Au₂{MeIm(CH₂)₃*tz*NHC}₂](PF₆)₂ and this can be ascribed to the absence of aurophilic interaction in complex **11**. The intramolecular Au...Au distance in **11** is in fact 6.2 Å longer than that observed in [Au₂{MeIm(CH₂)₃*tz*NHC}₂](PF₆)₂ (3.068 Å).

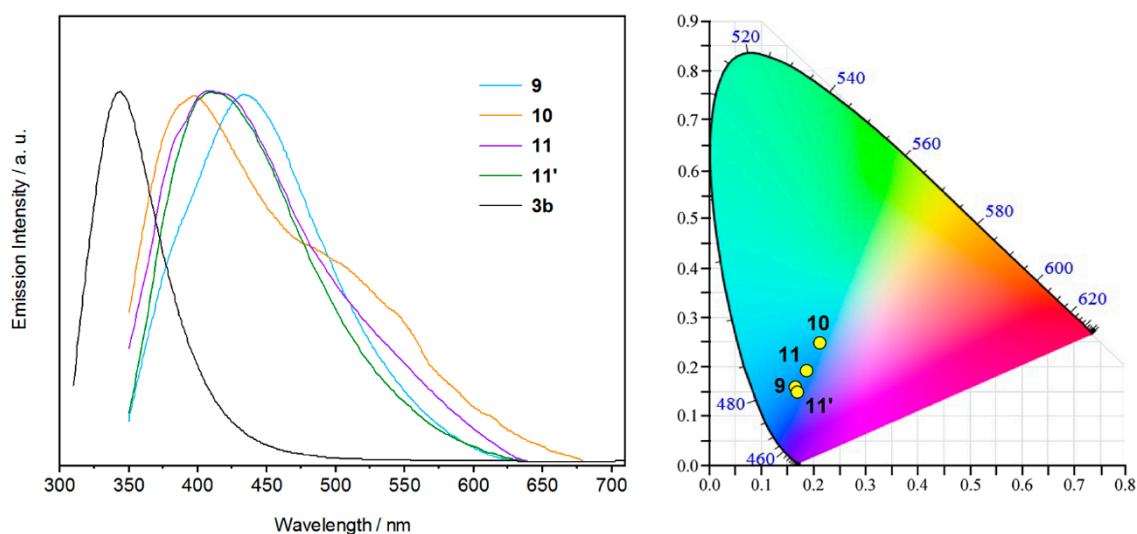


Figure 8. PL spectra of ligand **3b** and complexes **9**, **10**, **11** and **11'** obtained exciting the sample with UV light at 330 nm. The color coordinates calculated from the emission spectra are reported in the CIE1931 chromaticity diagram.

3. Materials and Methods

All manipulations and synthesis were carried out using standard Schlenk techniques under inert atmosphere of argon, or in a dry box MBraun Labmaster operating in dinitrogen atmosphere. The reagents and solvents were purchased as high-purity products and used as received. 1-mesityl-1H-imidazole was synthesized according to a procedure published in the literature [45]. NMR spectra were recorded at room temperature (298 K) on a Bruker Avance 300 MHz spectrometer (300.1 MHz for ^1H , 75.5 MHz for ^{13}C); chemical shifts (δ) are reported in ppm relative to the residual solvent signals. The ESI-MS analysis was performed using a Thermo-Finnigan LCQ-Duo (San Jose, CA, USA) cooperating in positive mode. The elemental analysis was carried out with a Thermo Scientific FLASH 2000 apparatus.

3.1. Synthesis of the Imidazolium Proligands

3.1.1. Synthesis of the Alkynyl Imidazolium Salts **1a** and **1b**

The proper N-substituted imidazole (3.0 mmol; 0.24 mL of N-methylimidazole or 0.56 g of N-mesitylimidazole), NaI (0.51 g, 3.4 mmol), 5-chloro-1-pentyne (0.5 mL, 4.7 mmol) and 10 mL of CH_3CN were introduced in a round bottom flask. The mixture was stirred under reflux for 24 h, then the solvent was removed under vacuum and the residue was treated with 10 mL of dichloromethane. The obtained mixture was filtered over Celite and the solution evaporated to dryness. **1a**. Orange solid (yield 70%). $^1\text{H-NMR}$ (300 MHz, CDCl_3) δ 9.85 (s, 1H, NCHN), 7.58 (s, 1H, CH_{im}), 7.55 (s, 1H, CH_{im}), 4.48 (m, 2H, NCH_2), 4.09 (s, 3H, NCH_3), 2.31 (m, 2H, CH_2C), 2.16 (m, 2H, CH_2), 2.10 (m, 1H, $\text{CH}_{\text{alkyne}}$). $^{13}\text{C-NMR}$ (75 MHz, CDCl_3) δ 136.9 (NCHN), 123.8 (CH_{im}), 122.7 (CH_{im}), 81.5 (C_{alkyne}), 71.2 (C_{alkyne}), 48.7 (NCH_2), 37.3 (NCH_3), 28.6 (CH_2), 15.5 (CH_2).

1b. Brown oil (yield 99%). $^1\text{H-NMR}$ (300 MHz, CD_3CN) δ 9.66 (s, 1H, NCHN), 8.08 (s, 1H, CH_{im}), 7.66 (s, 1H, CH_{im}), 7.06 (s, 2H, $\text{CH}_{\text{Mesityl}}$), 4.53 (m, 2H, NCH_2), 2.41 (m, 1H, $\text{CH}_{\text{alkyne}}$), 2.26 (m, 2H, CH_2C), 2.23 (s, 3H, $\text{Me}_{\text{Mesityl}}$), 2.14 (m, 2H, CH_2), 2.02 (s, 6H, $\text{Me}_{\text{Mesityl}}$). $^{13}\text{C-NMR}$ (75 MHz, CD_3CN) δ 141.4 ($\text{C}_{\text{Mesityl}}$), 137.8 (NCHN), 135.1 ($\text{C}_{\text{Mesityl}}$), 131.5 ($\text{C}_{\text{Mesityl}}$), 130.1 ($\text{C}_{\text{Mesityl}}$), 124.6 (CH_{im}), 124.1 (CH_{im}), 82.8 (C_{alkyne}), 71.8 (C_{alkyne}), 49.4 (NCH_2), 29.2 (CH_2), 21.3 ($\text{Me}_{\text{Mesityl}}$), 18.1 ($\text{Me}_{\text{Mesityl}}$), 15.8 (CH_2).

3.1.2. Synthesis of Proligands **2a** and **2b**

CuSO₄·5H₂O (0.10 g, 0.4 mmol), sodium ascorbate (0.12 g, 0.6 mmol) and 7 mL of CH₃CN were introduced in an ACE pressure tube. The mixture was stirred at room temperature for half an hour and then the proper alkynyl-imidazolium salt **1a** or **1b** (0.4 mmol) was added; the resulting mixture was further stirred at room temperature for one hour. Finally, phenylazide (0.80 mL of a 0.5 M solution in *t*-butylmethylether, 0.4 mmol) was added and the mixture was left under stirring at 60 °C for 24 h. The resulting mixture was filtered and the addition of KI (0.13 g, 0.8 mmol) to the filtrate caused extra precipitation of a white solid, which was filtered. The filtrate was evaporated under vacuum to remove the volatiles. The oily residue was dissolved in dichloromethane (ca. 15 mL), washed with aqueous ammonia (15 mL), water (5 mL) and finally dried over Na₂SO₄. Removal of the volatiles afforded the desired products. **2a**. Slightly yellow oil. ¹H-NMR (300 MHz, CDCl₃) δ 8.86 (s, 1H, NCHN), 8.01 (s, 1H, CH_{tz}), 7.75 (d, *J* = 7.8 Hz, 2H, ArH), 7.60–7.34 (m, 4H, ArH + CH_{im}), 7.19 (s, 1H, CH_{im}), 4.33 (m, 2H, NCH₂), 3.93 (s, 3H, NCH₃), 2.87 (m, 2H, CH₂C), 2.38 (m, 2H, CH₂). ESI-MS (positive ions, CH₃CN): *m/z* 268.05 ([**2a**-I]⁺). **2b**. Very hygroscopic yellow solid (yield 55%). ¹H-NMR (300 MHz, CD₃CN) δ 9.20 (s, 1H, NCHN), 8.35 (s, 1H, CH_{tz}), 7.83 (m, 3H, ArH + CH_{im}), 7.63–7.34 (m, 4H, ArH + CH_{im}), 7.07 (s, 2H, CH_{Mesityl}), 4.47 (m, 2H, NCH₂), 2.85 (m, 2H, CH₂C), 2.43 (m, 2H, CH₂), 2.38 (s, 3H, Me_{Mesityl}), 2.04 (s, 6H, Me_{Mesityl}). ¹³C-NMR (75 MHz, CD₃CN) δ 147.5 (C_{tz}), 142.0 (C_{Mesityl}), 138.0 and 137.8 (NCHN + C_{Mesityl}), 135.6 (C_{Mesityl}), 131.8 (C_{Mesityl}), 130.7 (ArH), 130.3 (CH_{Mesityl}), 129.4 (ArH), 124.8 (CH_{im}), 124.2 (CH_{im}), 121.6 (CH_{tz}), 121.0 (ArH), 50.0 (NCH₂), 29.9 (CH₂), 22.6 (CH₂C), 21.1 (Me_{Mesityl}), 17.6 (Me_{Mesityl}). ESI-MS (positive ions, CH₃CN): *m/z* 372.08 (100% [**2b**-I]⁺).

3.1.3. Synthesis of Proligand **3b**

MeI (0.2 mL, 3.4 mmol) was added to an acetonitrile solution (5 mL) of imidazolium salt **2b** (0.17 g, 0.34 mmol); the resulting solution was stirred under reflux for 12 h. The solvent was then removed under vacuum giving a dark brown solid, which was dissolved in MeOH (5 mL) and treated with a solution of KPF₆ (0.32 g, 1.7 mmol) in water (5 mL). The formed brownish precipitate was filtered and dried under vacuum. Brownish solid (yield 58%) ¹H-NMR (300 MHz, CD₃CN) δ 8.76 and 8.72 (2s, 2H, NCHN+CH_{tz}), 7.88 (m, 2H, ArH), 7.73 (m, 4H, ArH+CH_{im}), 7.51 (s, 1H, CH_{im}), 7.13 (s, 2H, CH_{Mesityl}), 4.42 (m, 2H, NCH₂), 4.26 (s, 3H, Me_{tz}), 2.97 (m, 2H, CH₂C), 2.42 (m, 2H, CH₂), 2.36 (s, 3H, Me_{Mesityl}), 2.06 (s, 6H, Me_{Mesityl}). ¹³C-NMR (75 MHz, CD₃CN) δ 144.7 (C_{tz}), 142.3 (C_{Mesityl}), 137.4 (NCHN), 135.7 (Ar and C_{Mesityl}), 132.9 (ArH), 131.8 (C_{Mesityl}), 131.5 (ArH), 130.4 (CH_{Mesityl}), 127.7 (CH_{tz}), 125.3 (CH_{im}), 124.2 (CH_{im}), 122.5 (ArH), 49.7 (NCH₂), 39.0 (Me_{tz}), 27.7 (CH₂C), 21.1 and 21.0 (CH₂ + Me_{Mesityl}), 17.5 (Me_{Mesityl}). ESI-MS (positive ions, CH₃CN): *m/z* 372.14 ([**3b**-2PF₆-CH₃]⁺), 532.08 ([**3b**-PF₆]⁺). Colourless needle-like crystals were obtained by slow diffusion of diethyl ether into an acetonitrile solution of the salt.

3.2. Synthesis of the Gold(I) Mononuclear Complexes

3.2.1. Synthesis of Complex **4**

In a round bottom flask were introduced K₂CO₃ (2.3 g, 16 mmol), 1-methyl-3-(pent-4-yn-1yl)-1*H*-imidazol-3-ium iodide (0.19 g, 0.68 mmol), AuCl(SMe₂) (0.10 g, 0.34 mmol) and 50 mL of dichloromethane. The mixture was left under stirring for four days at room temperature and then filtered. The filtrate was concentrated under reduced pressure to ca. 1–2 mL, then the addition of diethyl ether causes the formation of a white solid that was filtered. White solid (yield 60%). Anal. Calcd for C₁₈H₂₄N₄AuI: C 34.85, H 3.90, N 9.03%. Found: C 34.44, H 4.11, N 8.53%. ¹H-NMR (300 MHz, CD₃CN) δ 7.22 (d, *J* = 1.8 Hz, 1H, CH_{im}), 7.18 (d, *J* = 1.8 Hz, 1H, CH_{im}), 4.30 (t, *J* = 7.0 Hz, 2H, NCH₂), 3.85 (s, 3H, NCH₃), 2.23 (m, 3H, CH₂ + CH), 2.07 (m, 2H, CH₂). ¹³C-NMR (75 MHz, CD₃CN) δ 185.0 (CAu), 124.0 (CH_{im}), 122.5 (CH_{im}), 83.6 (C_{alkyne}), 71.0 (C_{alkyne}), 50.4 (NCH₂), 38.5 (NCH₃), 30.8 (CH₂), 15.9 (CH₂). ESI-MS (positive ions, CH₃CN): *m/z* 493.12 (100%, [**4**-I]⁺). Colourless crystals were obtained by slow diffusion of diethyl ether in a solution of the complex in acetonitrile.

3.2.2. Synthesis of Complex 5 and Characterization of Complex 7

In a round bottom flask were introduced proligand **2a** (0.11 g, 0.28 mmol), K_2CO_3 (1.24 g, 8.97 mmol), $AuCl(SMe_2)$ (0.042 g, 0.14 mmol) and 10 mL of acetonitrile; the mixture was left under stirring for 3 days and then filtered to remove the inorganic salts. The volatiles were evaporated, and the yellow solid was recrystallized from acetonitrile/diethyl ether. 1H -NMR (300 MHz, CD_3CN) δ 8.19 (s, 1H, CH_{tz}), 7.70 (m, 2H, ArH), 7.54–7.35 (m, 3H, ArH), 7.20 (d, $J = 1.8$ Hz, 1H, CH_{im}), 7.09 (d, $J = 1.8$ Hz, 1H, CH_{im}), 4.22 (t, $J = 7.0$ Hz, 2H, NCH_2), 3.73 (s, 3H, NCH_3), 2.73 (t, $J = 7.0$ Hz, 2H, CH_2), 2.27 (m, 2H, CH_2). ^{13}C -NMR (75 MHz, CD_3CN) δ 184.8 (CAu), 147.8 (C_{tz}), 137.9 (Ar), 130.7 (ArH), 129.2 (ArH), 123.9 (CH_{im}), 122.2 (CH_{im}), 121.1 (CH_{tz}), 120.6 (ArH), 50.6 (NCH_2), 38.4 (NCH_3), 30.8 (CH_2), 22.6 (CH_2C). ESI-MS (positive ions, CH_3CN): m/z 731.23 (100%, $[5-I]^+$).

The first attempt for the synthesis of complex **5** was performed for 4 days with a sample of proligand **2a** containing some copper impurities. The 1H -NMR spectrum of the solid isolated from this attempt shows the presence of two sets of signals, attributed to complexes **5** and **7** in a ratio ca. 60(5):40(7). The identity of complex **7** was clarified by X-ray diffraction analysis of some crystals obtained from the acetonitrile/diethyl ether mother liquor of the final filtration. NMR signals of **7** have been assigned in the 1H -NMR of the crude mixture by exclusion of the signals attributed to **5**. 1H -NMR (300 MHz, CD_3CN) δ 8.11 (s, 1H, CH_{tz}), 7.81 (m, 2H, ArH), 7.60–7.30* (m, 3H, ArH), 7.20 (d, 1H, CH_{im}), 7.11 (d, 1H, CH_{im}), 4.25* (m, 2H, NCH_2), 3.76 (s, CH_3), 2.78* (m, 2H, CH_2), 2.25* (m, 2H, CH_2). * signals superimposed with those of complex **5**.

3.2.3. Synthesis of Complex 6

In a round bottom flask were introduced K_2CO_3 (1.5 g, 11 mmol), proligand **2b** (0.23 g, 0.45 mmol), $AuCl(SMe_2)$ (0.065 g, 0.22 mmol) and 10 mL of acetonitrile. The mixture was left under stirring for 2 days at room temperature and then filtered. The volatiles were evaporated from the filtrate and the white residue was recrystallized from acetonitrile/diethyl ether, filtered and dried under vacuum. Off-white solid (yield 74%). 1H -NMR (300 MHz, CD_3CN) δ 8.11 (s, 1H, CH_{tz}), 7.77 (d, $J = 7.4$ Hz, 2H, ArH), 7.55 (m, 2H, ArH), 7.46 (m, 1H, ArH), 7.43 (d, $J = 1.8$ Hz, 1H, CH_{im}), 7.07 (d, $J = 1.8$ Hz, 1H, CH_{im}), 6.94 (s, 2H, $CH_{Mesityl}$), 4.15 (m, 2H, NCH_2), 2.64 (m, 2H, CH_2C), 2.31 (s, 3H, $Me_{Mesityl}$), 1.77 (s, 6H, $Me_{Mesityl}$), the missing CH_2 signal is covered by the signal of water (s, 2.23). ^{13}C -NMR (75 MHz, CD_3CN) δ 184.9 (CAu), 148.0 (C_{tz}), 140.4 ($C_{Mesityl}$), 138.1 (CAr), 135.9 ($C_{Mesityl}$), 130.7 (ArH), 130.6 ($C_{Mesityl}$), 129.8 ($CH_{Mesityl}$), 129.4 (ArH), 123.8 (CH_{im}), 123.1 (CH_{im}), 121.0 (ArH), 120.9 (CH_{tz}), 51.0 (NCH_2), 31.4 (CH_2), 23.0 (CH_2C), 21.1 ($Me_{Mesityl}$), 17.6 ($Me_{Mesityl}$). ESI-MS (positive ions, CH_3CN): m/z 939.27 (100%, $[6-I]^+$). Yellowish crystals were obtained by slow diffusion of diethyl ether into a solution of the complex in an acetonitrile/hexane mixture.

3.2.4. Synthesis of Complex 8 by Methylation of Complex 6

Complex **6** (0.15 g, 0.14 mmol) was introduced in a round bottom flask and then transferred in a dry box, where the solid was dissolved in 3 mL of dry acetonitrile. Solid Me_3OBF_4 (0.047 g, 0.32 mmol) was added to the solution of complex **6** and the mixture was left stirring for 2 h at room temperature. When the reaction was completed, the volume of acetonitrile was reduced under vacuum. The opaque yellow solution was filtered; the addition of diethyl ether gives an off-white solid that deposits at the bottom of the flask and forms gradually a yellowish oil. The ether was removed and the oil was treated under vacuum forming a white solid (yield 99%). 1H -NMR (300 MHz, CD_3CN) δ 8.74 (s, 1H, CH_{tz}), 7.87 (m, 2H, ArH), 7.69 (m, 3H, ArH), 7.50 (d, $J = 1.9$ Hz, 1H, CH_{im}), 7.12 (d, $J = 1.9$ Hz, 1H, CH_{im}), 6.99 (s, 2H, $CH_{Mesityl}$), 4.32 (m, 2H, NCH_2), 4.20 (s, 3H, NCH_3), 2.85 (m, 2H, CH_2C), 2.38 (s, 3H, $Me_{Mesityl}$), 2.33 (m, 2H, CH_2), 1.78 (s, 6H, $Me_{Mesityl}$). ^{13}C -NMR (75 MHz, CD_3CN) δ 184.9 (CAu), 145.1 (C_{tz}), 140.4 ($C_{Mesityl}$), 135.8 ($C_{Mesityl}$), 135.7 (CAr), 132.8 (ArH), 131.4 (ArH), 131.2 ($C_{Mesityl}$), 129.9 ($CH_{Mesityl}$), 127.4 (CH_{tz}), 124.3 (CH_{im}), 123.0 (CH_{im}), 122.4 (ArH), 50.5 (NCH_2), 38.6 (NCH_3), 28.9

(CH₂), 21.2 and 21.0 (CH₂C+Me_{Mesityl}), 17.6 (Me_{Mesityl}). ESI-MS (positive ions, CH₃CN): *m/z* 1143.33 ([8-I]⁺), 323.36 ([8-2BF₄-I]³⁺).

3.3. Synthesis of the Dinuclear Complexes with Bridging Dicarbene Ligands

3.3.1. Synthesis of Complex 9

Complex 8 (0.17 g, 0.14 mmol), Ag₂O (0.072 g, 0.31 mmol) and 5 mL of acetonitrile were introduced in an ACE pressure tube, that was then closed and the mixture was heated at 40 °C for 24 h. Then the mixture was filtered using a PTFE filter (0.45 μm) and a syringe. The solvent was finally removed under vacuum and the flask transferred in a dry box; the residue was dissolved in the minimum amount of dry acetonitrile and diethyl ether was added, affording the precipitation of a white solid. Unfortunately, the solid darkens with time. ¹H-NMR (300 MHz, CD₃CN) δ 7.90–7.34 (m, 5H, ArH + CH_{im}), 7.08 (d, *J* = 1.8 Hz, 1H, CH_{im}), 6.91 (s, 2H, CH_{Mesityl}), 4.16 (m, 5H, NCH₂ + NCH₃), 2.80 (m, 2H, CH₂C), 2.35 (s, 3H, Me_{Mesityl}), 2.22 (m, 2H, CH₂C), 1.67 (s, 6H, Me_{Mesityl}). ¹³C-NMR (75 MHz, CD₃CN) δ 184.0 (C_{im}Au), 165.1 (C_{tz}Au), 148.7 (C_{tz}), 141.0 (C_{Ar}), 140.3 (C_{Mesityl}), 135.7 (C_{Mesityl}), 131.3 (ArH), 130.6 (ArH), 129.9 (C_{Mesityl}), 129.7 (CH_{Mesityl}), 124.5 (ArH), 123.9 (CH_{im}), 123.3 (CH_{im}), 50.5 (NCH₂), 37.2 (NCH₃), 30.6 (CH₂), 22.7 (CH₂C), 21.1 (Me_{Mesityl}), 17.5 (Me_{Mesityl}). ESI-MS (positive ions, CH₃CN): *m/z* 1161 and 1163.25 (100% [5-BF₄]⁺).

3.3.2. Synthesis of Complex 10

Proligand 3b (0.083 g, 0.15 mmol) and Ag₂O (0.095 g, 0.41 mmol) were introduced in a Schlenk tube under inert atmosphere and CH₃CN (5 mL) was added. The dark mixture was left under stirring for one night at 80 °C. The mixture was filtered with a PTFE filter (0.45 μm) with a syringe, obtaining a clear solution; evaporation of volatiles affords an off-white solid, which darkens with time. ¹H-NMR (300 MHz, CD₃CN) δ 7.63–7.31 (m, 6H, ArH + CH_{im}), 7.14 (s, 1H, CH_{im}), 6.94 (s, 2H, CH_{Mesityl}), 4.13 (br, 5H, NCH₂ + NCH₃), 2.78 (m, 2H, CH₂), 2.31 (s, 3H, Me_{Mesityl}), 2.22 (m, 2H, CH₂C), 1.75 (br, 6H, Me_{Mesityl}). ¹³C-NMR (75 MHz, CD₃CN) δ 148.7 (C_{tz}), 140.9 (C_{Ar}), 140.3 (C_{Mesityl}), 136.5 (C_{Mesityl}), 135.8 (ArH), 131.2 (ArH), 130.6 (ArH), 130.0 (C_{Mesityl}), 129.9 (CH_{Mesityl}), 124.2 (CH_{im}), 122.9 (CH_{im}), 51.0 (NCH₂), 37.3 (NCH₃), 30.8 (CH₂), 22.7 (CH₂C), 21.0 (Me_{Mesityl}), 17.7 (Me_{Mesityl}). C_{tz}Ag carbene signal was detected in the 2D ¹³C, ¹H HMBC-NMR spectra at 175.7 ppm; C_{im}Au not detected. ESI-MS (positive ions, CH₃CN): *m/z* 492.21 ([Ag(diNHC)]⁺), 1131.04 ([10-PF₆]⁺) with diNHC = *n*NHC-*tz*NHC.

3.3.3. Synthesis of Complexes 11/11'

Proligand 3b (0.083 g, 0.15 mmol) and Ag₂O (0.095 g, 0.41 mmol), were introduced in a Schlenk tube and, after making an inert atmosphere, CH₃CN (5 mL) was added. The dark mixture was left under stirring for one night at 80 °C. Precursor AuCl(SMe₂) (0.036 g, 0.12 mmol) was then added to the mixture and a white-purplish solid formed. After two hours stirring, the mixture was filtered with a PTFE filter (0.45 μm) with a syringe, obtaining a clear solution; evaporation of volatiles affords an off-white solid; the residue was dissolved in the minimum amount of dry acetonitrile and diethyl ether was added, affording the precipitation of a white solid (yield 60%). The ¹H-NMR shows two main species presents in roughly the same quantity, which are two isomeric forms of the gold complex (11/11'). ESI-MS (positive ions, CH₃CN): *m/z* 1309.18 ([11/11'-PF₆]⁺). 11. ¹H-NMR (300 MHz, CD₃CN) δ 7.70–7.30 (m, 6H, ArH + CH_{im}), 7.16 (d, *J* = 1.8 Hz, 1H, CH_{im}), 6.97 (s, 2H, CH_{Mesityl}), 4.40 (m, 2H, NCH₂), 4.12 (s, 3H, NCH₃), 2.89 (m, 2H, CH₂C), 2.38 (m, 2H, CH₂), 2.31 (s, 3H, Me_{Mesityl}), 1.86 (s, 6H, Me_{Mesityl}). ¹³C-NMR (75 MHz, CD₃CN) δ 185.3 (C_{im}Au), 169.8 (C_{tz}Au), 148.5 (C_{tz}), 140.5 (C_{Mesityl}), 139.7 (C_{Ar}), 135.7 (C_{Mesityl}), 131.2 (ArH), 130.5 (ArH), 130.0 (CH_{Mesityl}), 125.1 (ArH), 124.3 (C_{Mesityl}), 124.1 (CH_{im}), 122.7 (CH_{im}), 51.1 (NCH₂), 37.8 (NCH₃), 30.7 (CH₂), 23.0 (CH₂C), 21.0 (Me_{Mesityl}), 17.8 (Me_{Mesityl}). 11'. ¹H-NMR (300 MHz, CD₃CN) δ 7.80–7.34 (m, 6H, ArH and CH_{im}), 7.08 (d, *J* = 1.8 Hz, 1H, CH_{im}), 6.92 (s, 2H, CH_{Mesityl}), 4.24 (m, 2H, NCH₂), 4.14 (s, 3H, NCH₃), 2.86 (m, 2H, CH₂C), 2.37 (s, 3H, Me_{Mesityl}), 2.35 (m, 2H, CH₂), 1.67 (s, 6H, Me_{Mesityl}). ¹³C-NMR (75 MHz, CD₃CN) δ 184.3 (C_{im}Au),

170.9 (C_{tzAu}), 148.3 (C_{tz}), 140.4 ($C_{Mesityl}$), 140.1 (C_{Ar}), 135.6 ($C_{Mesityl}$), 131.5 (ArH), 130.5 (ArH), 129.8 ($CH_{Mesityl}$), 125.1 (ArH), 124.2 (CH_{im}), 124.1 ($C_{Mesityl}$), 123.0 (CH_{im}), 50.7 (NCH_2), 37.8 (NCH_3), 30.4 (CH_2), 22.7 (CH_2C), 21.1 ($Me_{Mesityl}$), 17.5 ($Me_{Mesityl}$).

3.4. Crystal Structure Determination

Data were collected using an Oxford Diffraction Gemini E diffractometer, equipped with a 2K × 2K EOS CCD area detector and sealed-tube Enhance (Mo) and (Cu) X-ray sources. Single crystals of compounds have been fastened on the top of a Lindemann glass capillary. Data have been collected by means of the ω -scans technique using graphite-monochromated radiation. Detector distance has been set at 45 mm. The diffraction intensities have been corrected for Lorentz/polarization effects, as well as with respect to absorption. Empirical multi-scan absorption corrections using equivalent reflections have been performed with the scaling algorithm SCALE3 ABSPACK. Data reduction, finalization and cell refinement were carried out through the CrysAlisPro software (1.171.38.46, Rigaku Oxford Diffraction, Rigaku Corporation, Oxford, UK: 2015). Accurate unit cell parameters were obtained by least squares refinement of the angular settings of strongest reflections, chosen from the whole experiment. The structures were solved with Olex2 [46] by using ShelXT [47] structure solution program by Intrinsic Phasing and refined with the ShelXL [48] refinement package using least-squares minimization. In the last cycles of refinement, non-hydrogen atoms were refined anisotropically. Hydrogen atoms were included in calculated positions, and a riding model was used for their refinement. The specific refinement details for each of the compounds are embedded in their CIF files that have been deposited with the Cambridge Crystallographic Data Centre as supplementary publication (CCDC 1903103-1903107). Copies of the data can be obtained free of charge on application to the CCDC, 12 Union Road, Cambridge CB2 1EZ, U.K. (fax, (+44) 1223 336033; e-mail, deposit@ccdc.cam.ac.uk).

3.5. Luminescence Measurements

The luminescence spectra of films obtained by drop-casting from acetonitrile solutions on quartz slides were recorded at room temperature using a Fluorolog-3, Horiba JobinYvon spectrofluorimeter equipped with double-grating monochromator in both the excitation and emission sides. A 450 W Xe arc lamp and an R928P Hamamatsu photomultiplier were employed as excitation source and detector, respectively. The emission spectra were corrected for detection and optical spectral response of the spectrofluorimeter supplied by the manufacturer.

4. Conclusions

In this work, different strategies for the synthesis of heterobimetallic complexes with heteroditopic *n*NHC-*tz*NHC carbene ligands were explored. The best results were obtained with a three-step procedure involving: (i) Metal coordination of an *n*NHC functionalized with a triazole pendant ring; (ii) methylation of the triazole ring; and (iii) coordination of the *tz*NHC to a second and different metal center. The Au-Ag bimetallic complex synthesized in this way can be the precursor of other bimetallic Au-M (M = transition metal center other than Au) complexes, via transmetalation reactions and we are currently exploring this reactivity.

The approach described in this work for the synthesis of heterobimetallic complexes appears quite general, since it could be applied to a broad class of ligands, as long as the proper azolium-pendant azole precursor could be isolated [35,49–51].

Supplementary Materials: The following are available online, Figures S1–S25: 1H - and ^{13}C -NMR spectra of the new compounds synthesized in this work. Table S1: crystal data and structure refinement for compounds **3b**, **4**, **6**, **7** and **11**. Cif and checkcif files of the crystal structures.

Author Contributions: Conceptualization, C.T.; validation, A.L. and C.T.; investigation, A.L., M.R., G.B. and P.S.; resources, C.T.; data curation, A.L., M.R. and G.B.; writing—original draft preparation, A.L. and C.T.; writing—review and editing, all authors; visualization, A.L., M.B., M.R. and G.B.; supervision, C.T.

Funding: This research was funded by Università degli Studi di Padova (Progetto di Ricerca di Ateneo CPDA20140431). APC was sponsored by MDPI.

Conflicts of Interest: The authors declare no conflict of interest.

References

1. Arduengo, A.J.; Harlow, R.L.; Kline, M. A stable crystalline carbene. *J. Am. Chem. Soc.* **1991**, *113*, 361–363. [[CrossRef](#)]
2. Huynh, H.V. *The Organometallic Chemistry of N-Heterocyclic Carbenes*; John Wiley & Sons, Inc.: Hoboken, NJ, USA, 2017.
3. Peris, E. Smart N-Heterocyclic Carbene Ligands in Catalysis. *Chem. Rev.* **2018**, *118*, 9988–10031. [[CrossRef](#)] [[PubMed](#)]
4. Nolan, S.P. *N-Heterocyclic Carbenes, Effective Tools for Organometallic Synthesis*; Wiley-VCH: Weinheim, Germany, 2014.
5. Diez-Gonzalez, S. *N-Heterocyclic Carbenes: From Laboratory Curiosities to Efficient Synthetic Tools*, 2nd ed.; RSC Catalysis Series; RSC: Cambridge, UK, 2017.
6. Biffis, A.; Tubaro, C.; Baron, M. Advances in Transition-Metal-Catalysed Alkyne Hydroarylations. *Chem. Rev.* **2016**, *16*, 1742–1760. [[CrossRef](#)] [[PubMed](#)]
7. Vivancos, A.; Segarra, C.; Albrecht, M. Mesoionic and Related Less Heteroatom-Stabilized N-Heterocyclic Carbene Complexes: Synthesis, Catalysis, and Other Applications. *Chem. Rev.* **2018**, *118*, 9493–9586. [[CrossRef](#)]
8. Visbal, R.; Gimeno, M.C. N-heterocyclic carbene metal complexes: Photoluminescence and applications. *Chem. Soc. Rev.* **2014**, *43*, 3551–3574. [[CrossRef](#)] [[PubMed](#)]
9. Merics, L.; Albrecht, M. Beyond catalysis: N-heterocyclic carbene complexes as components for medicinal, luminescent, and functional materials applications. *Chem. Soc. Rev.* **2010**, *39*, 1903–1912. [[CrossRef](#)] [[PubMed](#)]
10. Oehninger, L.; Rubbiani, R.; Ott, I. N-Heterocyclic carbene metal complexes in medicinal chemistry. *Dalton Trans.* **2013**, *42*, 3269–3284. [[CrossRef](#)] [[PubMed](#)]
11. Liu, W.; Gust, R. Update on metal N-heterocyclic carbene complexes as potential anti-tumor metallodrugs. *Coord. Chem. Rev.* **2016**, *329*, 191–213. [[CrossRef](#)]
12. Mora, M.; Gimeno, M.C.; Visbal, R. Recent advances in gold–NHC complexes with biological properties. *Chem. Soc. Rev.* **2019**, *48*, 447–462. [[CrossRef](#)]
13. Biffis, A.; Baron, M.; Tubaro, C. Chapter five-Poly-NHC complexes of transition metals: recent applications and new trends. In *Advances in Organometallic Chemistry*; Pérez, P.J., Ed.; Academic Press: Cambridge, MA, USA, 2015; pp. 203–288.
14. Schmidbaur, H.; Schier, A. A briefing on aurophilicity. *Chem. Soc. Rev.* **2008**, *37*, 1931–1951. [[CrossRef](#)]
15. Baron, M.; Tubaro, C.; Biffis, A.; Basato, M.; Graiff, C.; Poater, A.; Cavallo, L.; Armaroli, N.; Accorsi, G. Blue-Emitting Dinuclear N-heterocyclic Dicarbene Gold(I) Complex Featuring a Nearly Unit Quantum Yield. *Inorg. Chem.* **2012**, *51*, 1778–1784. [[CrossRef](#)] [[PubMed](#)]
16. Ghimire, M.M.; Nesterov, V.N.; Omary, M.A. Remarkable Aurophilicity and Photoluminescence Thermochromism in a Homoleptic Cyclic Trinuclear Gold(I) Imidazolate Complex. *Inorg. Chem.* **2017**, *56*, 12086–12089. [[CrossRef](#)] [[PubMed](#)]
17. Penney, A.A.; Sizov, V.V.; Grachova, E.V.; Krupenya, D.V.; Gurzhiy, V.V.; Starova, G.L.; Tunik, S.P. Aurophilicity in Action: Fine-Tuning the Gold(I)–Gold(I) Distance in the Excited State to Modulate the Emission in a Series of Dinuclear Homoleptic Gold(I)–NHC Complexes. *Inorg. Chem.* **2016**, *55*, 4720–4732. [[CrossRef](#)] [[PubMed](#)]
18. Mata, J.A.; Hahn, F.E.; Peris, E. Heterometallic complexes, tandem catalysis and catalytic cooperativity. *Chem. Sci.* **2014**, *5*, 1723–1732. [[CrossRef](#)]
19. Böhmer, M.; Kampert, F.; Tan, T.T.Y.; Guisado-Barrios, G.; Peris, E.; Hahn, F.E. Ir^{III}/Au^I and Rh^{III}/Au^I Heterobimetallic Complexes as Catalysts for the Coupling of Nitrobenzene and Benzylic Alcohol. *Organometallics* **2018**, *37*, 4092–4099. [[CrossRef](#)]
20. Böhmer, M.; Guisado-Barrios, G.; Kampert, F.; Roelfes, F.; Tan, T.T.Y.; Peris, E.; Hahn, F.E. Synthesis and Catalytic Applications of Heterobimetallic Carbene Complexes Obtained via Sequential Metalation of Two Bisazolium Salts. *Organometallics* **2019**, *38*, 2120–2131. [[CrossRef](#)]

21. Schulte to Brinke, C.; Hahn, F.E. Trinuclear Heterobimetallic Complexes by Stepwise Metalation of a Macrocyclic Tetraimidazolium Salt. *Eur. J. Inorg. Chem.* **2015**, 3227–3231. [[CrossRef](#)]
22. Gonell, S.; Poyatos, M.; Peris, E. Pincer–CNC mononuclear, dinuclear and heterodinuclear Au(III) and Pt(II) complexes supported by mono- and poly-N-heterocyclic carbenes: Synthesis and photophysical properties. *Dalton Trans.* **2016**, 45, 5549–5556. [[CrossRef](#)]
23. Majumder, A.; Naskar, R.; Roy, P.; Maity, R. Homo- and Heterobimetallic Complexes Bearing NHC Ligands: Applications in α -Arylation of Amide, Suzuki–Miyaura Coupling Reactions, and Tandem Catalysis. *Eur. J. Inorg. Chem.* **2019**, 1810–1815. [[CrossRef](#)]
24. Teng, Q.; Huynh, H.V. (Hetero)bimetallic and Tetranuclear Complexes of Pincer-Bridged N-Heterocyclic Carbene Ligands. *Organometallics* **2018**, 37, 4119–4127. [[CrossRef](#)]
25. Zanardi, A.; Corberán, R.; Mata, J.A.; Peris, E. Homo- and Heterodinuclear Complexes with Triazolyl-diylidene. An Easy Approach to Tandem Catalysts. *Organometallics* **2008**, 27, 3570–3576. [[CrossRef](#)]
26. Wang, W.; Zhao, L.; Lv, H.; Zhang, G.; Xia, C.; Hahn, F.E.; Li, F. Modular “Click” Preparation of Bifunctional Polymeric Heterometallic Catalysts. *Angew. Chem. Int. Ed.* **2016**, 55, 7665–7670. [[CrossRef](#)] [[PubMed](#)]
27. Bente, S.; Kampert, F.; Tan, T.T.Y.; Hahn, F.E. Site-selective metallation of dicarbene precursors. *Chem. Commun.* **2018**, 54, 12887–12890. [[CrossRef](#)] [[PubMed](#)]
28. Monticelli, M.; Baron, M.; Tubaro, C.; Bellemin-Lapponnaz, S.; Graiff, C.; Bottaro, G.; Armelao, L.; Orian, L. Structural and Luminescent Properties of Homoleptic Silver(I), Gold(I), and Palladium(II) Complexes with nNHC-tzNHC Heteroditopic Carbene Ligands. *ACS Omega* **2019**, 4, 4192–4205. [[CrossRef](#)]
29. Zamora, M.T.; Ferguson, M.J.; McDonald, R.; Cowie, M. Unsymmetrical Dicarbene Complexes Based on N-Heterocyclic/Mesoionic Carbene Frameworks: A Stepwise Metalation Strategy for the Generation of a Dicarbene-Bridged Mixed-Metal Pd/Rh Complex. *Organometallics* **2012**, 31, 5463–5477. [[CrossRef](#)]
30. Nelson, D.J.; Nolan, S.P. Quantifying and understanding the electronic properties of N-heterocyclic carbenes. *Chem. Soc. Rev.* **2013**, 42, 6723–6753. [[CrossRef](#)] [[PubMed](#)]
31. Chardon, E.; Puleo, G.L.; Dahm, G.; Fournel, S.; Guichard, G.; Bellemin-Lapponnaz, S. Easy Derivatisation of Group 10 N-Heterocyclic Carbene Complexes and In Vitro Evaluation of an Anticancer Oestradiol Conjugate. *ChemPlusChem* **2012**, 77, 1028–1038. [[CrossRef](#)]
32. Mendoza-Espinosa, D.; Alvarez-Hernández, A.; Angeles-Beltrán, D.; Negrón-Silva, G.E.; Suárez-Castillo, O.R.; Vásquez-Pérez, J.M. Bridged N-Heterocyclic/Mesoionic (NHC/MIC) Heterodicarbene Complexes as Ligands for Transition Metal Complexes. *Inorg. Chem.* **2017**, 56, 2092–2099. [[CrossRef](#)]
33. Gaillard, S.; Nun, P.; Slawin, A.M.Z.; Nolan, S.P. Expedient Synthesis of [Au(NHC)(L)]⁺ (NHC = N-Heterocyclic Carbene; L = Phosphine or NHC) Complexes. *Organometallics* **2010**, 29, 5402–5408. [[CrossRef](#)]
34. Visbal, R.; Laguna, A.; Gimeno, M.C. Simple and efficient synthesis of [MCl(NHC)] (M = Au, Ag) complexes. *Chem. Commun.* **2013**, 49, 5642–5644. [[CrossRef](#)]
35. Baron, M.; Tubaro, C.; Basato, M.; Isse, A.A.; Gennaro, A.; Cavallo, L.; Graiff, C.; Dolmella, A.; Falivene, L.; Caporaso, L. Insights into the Halogen Oxidative Addition Reaction to Dinuclear Gold(I) Di(NHC) Complexes. *Chem. Eur. J.* **2016**, 22, 10211–10224. [[CrossRef](#)] [[PubMed](#)]
36. Pell, T.P.; Wilson, D.J.D.; Skelton, B.W.; Dutton, J.L.; Barnard, P.J. Heterobimetallic N-Heterocyclic Carbene Complexes: A Synthetic, Spectroscopic, and Theoretical Study. *Inorg. Chem.* **2016**, 55, 6882–6891. [[CrossRef](#)] [[PubMed](#)]
37. Tubaro, C.; Baron, M.; Costante, M.; Basato, M.; Biffis, A.; Gennaro, A.; Isse, A.A.; Graiff, C.; Accorsi, G. Dinuclear gold(I) complexes with propylene bridged N-heterocyclic dicarbene ligands: Synthesis, structures, and trends in reactivities and properties. *Dalton Trans.* **2013**, 42, 10952–10963. [[CrossRef](#)] [[PubMed](#)]
38. Keske, E.C.; Zenkina, O.V.; Wang, R.; Crudden, C.M. Synthesis and Structure of Silver and Rhodium 1,2,3-Triazol-5-ylidene Mesoionic Carbene Complexes. *Organometallics* **2012**, 31, 456–461. [[CrossRef](#)]
39. Huang, W.; Zhang, Y.-C.; Jin, R.; Chen, B.-L.; Chen, Z. Synthesis of Axially Chiral 1,2,3-Triazol-5-ylidene–Au(I) Complex and Its Application in Enantioselective [2 + 2] Cycloaddition of Alleneamides with Alkenes. *Organometallics* **2018**, 37, 3196–3209. [[CrossRef](#)]
40. Guisado-Barrios, G.; Bouffard, J.; Donnadiou, B.; Bertrand, G. Crystalline 1H-1,2,3-Triazol-5-ylidenes: New Stable Mesoionic Carbenes (MICs). *Angew. Chem. Int. Ed.* **2010**, 49, 4759–4762. [[CrossRef](#)]
41. Huynh, H.V.; Han, Y.; Jothibasu, R.; Yang, J.A. ¹³C-NMR Spectroscopic Determination of Ligand Donor Strengths Using N-Heterocyclic Carbene Complexes of Palladium(II). *Organometallics* **2009**, 28, 5395–5404. [[CrossRef](#)]

42. Huynh, H.V. Electronic Properties of N-Heterocyclic Carbenes and Their Experimental Determination. *Chem. Rev.* **2018**, *118*, 9457–9492. [[CrossRef](#)]
43. Hemmert, C.; Poteau, R.; dit Dominique, F.J.-B.; Ceroni, P.; Bergamini, G.; Gornitzka, H. Amide-Functionalized Bis(NHC) Systems: Anion Effect on Gold–Gold Interactions. *Eur. J. Inorg. Chem.* **2012**, *2012*, 3892–3898. [[CrossRef](#)]
44. Cure, J.; Poteau, R.; Gerber, I.C.; Gornitzka, H.; Hemmert, C. Dimeric Gold Bis(carbene) Complexes by Transmetalation in Water. *Organometallics* **2012**, *31*, 619–626. [[CrossRef](#)]
45. Strassner, T.; Ahrens, S. Salts comprising aryl-alkyl-substituted imidazolium and triazolium cations and the use thereof. Patent WO2009095012A1, 6 August 2009.
46. Dolomanov, O.V.; Bourhis, L.J.; Gildea, R.J.; Howard, J.a.K.; Puschmann, H. OLEX2: A complete structure solution, refinement and analysis program. *J. Appl. Crystallogr.* **2009**, *42*, 339–341. [[CrossRef](#)]
47. Sheldrick, G.M. SHELXT—Integrated space-group and crystal-structure determination. *Acta Crystallogr. Sect. Found. Adv.* **2015**, *71*, 3–8. [[CrossRef](#)] [[PubMed](#)]
48. Sheldrick, G.M. Crystal structure refinement with SHELXL. *Acta Crystallogr. Sect. C Struct. Chem.* **2015**, *71*, 3–8. [[CrossRef](#)] [[PubMed](#)]
49. Box, H.K.; Howell, T.O.; Kennon, W.E.; Burk, G.A.; Valle, H.U.; Hollis, T.K. An efficient route to unsymmetrical bis(azolium) salts: CCC-NHC pincer ligand complex precursors. *Tetrahedron* **2017**, *73*, 2191–2195. [[CrossRef](#)]
50. Aznarez, F.; Sanz Miguel, P.J.; Tan, T.T.Y.; Hahn, F.E. Preparation of Rhodium(III) Di-NHC Chelate Complexes Featuring Two Different NHC Donors via a Mild NaOAc-Assisted C–H Activation. *Organometallics* **2016**, *35*, 410–419. [[CrossRef](#)]
51. Monticelli, M.; Bellemin-Laponnaz, S.; Tubaro, C.; Rancan, M. Synthesis, Structure and Antitumoural Activity of Triazole-Functionalised NHC–Metal Complexes. *Eur. J. Inorg. Chem.* **2017**, *2017*, 2488–2495. [[CrossRef](#)]

Sample Availability: Samples of the compounds are not available from the authors.



© 2019 by the authors. Licensee MDPI, Basel, Switzerland. This article is an open access article distributed under the terms and conditions of the Creative Commons Attribution (CC BY) license (<http://creativecommons.org/licenses/by/4.0/>).